

## 非线性系统中双频光栅相位测量

乔闹生 尚雪

### Phase measurement with dual-frequency grating in a nonlinear system

QIAO Nao-sheng, SHANG Xue

引用本文:

乔闹生, 尚雪. 非线性系统中双频光栅相位测量[J]. *中国光学*, 2023, 16(3): 726–732. doi: 10.37188/CO.EN.2022–0013

QIAO Nao-sheng, SHANG Xue. Phase measurement with dual-frequency grating in a nonlinear system[J]. *Chinese Optics*, 2023, 16(3): 726–732. doi: 10.37188/CO.EN.2022–0013

在线阅读 View online: <https://doi.org/10.37188/CO.EN.2022–0013>

## 您可能感兴趣的其他文章

### Articles you may be interested in

#### 光学三维扫描仪光强传递函数的测量和校正

Measurement and calibration of the intensity transform function of the optical 3D profilometry system

*中国光学 (中英文)*. 2018, 11(1): 123 <https://doi.org/10.3788/CO.20181101.0123>

#### 基于数字相位恢复算法的正交相移键控自由空间相干光通信系统

Coherent free-space optical communication system with quadrature phase-shift keying modulation using a digital phase recovery algorithm

*中国光学 (中英文)*. 2019, 12(5): 1131 <https://doi.org/10.3788/CO.20191205.1131>

#### 纳米尺度下的局域场增强研究进展

Advances in the local field enhancement at nanoscale

*中国光学 (中英文)*. 2018, 11(1): 31 <https://doi.org/10.3788/CO.20181101.0031>

#### 基于彩色编码光栅投影的双N步相移轮廓术

Double N-step phase-shifting profilometry using color-encoded grating projection

*中国光学 (中英文)*. 2019, 12(3): 616 <https://doi.org/10.3788/CO.20191203.0616>

#### 基于衍射光栅的干涉式精密位移测量系统

Interferometric precision displacement measurement system based on diffraction grating

*中国光学 (中英文)*. 2017, 10(1): 39 <https://doi.org/10.3788/CO.20171001.0039>

#### 用于智能移动设备的条纹反射法检测系统

Deflectometry measurement system for smart mobile devices

*中国光学 (中英文)*. 2017, 10(2): 267 <https://doi.org/10.3788/CO.20171002.0267>

文章编号 2097-1842(2023)03-0726-07

## Phase measurement with dual-frequency grating in a nonlinear system

QIAO Nao-sheng<sup>1,2\*</sup>, SHANG Xue<sup>2</sup>

(1. International College, Hunan University of Arts and Science, Changde 415000, China;

2. Mathematics and Physics Science College, Hunan University of Arts and Science,  
Changde 415000, China)

\* Corresponding author, E-mail: naoshengqiao@163.com

**Abstract:** To gain better phase measurement results in nonlinear measurement systems, a phase measurement method that uses dual-frequency grating after reducing the nonlinear effect is proposed. Firstly, the nonlinear effect of the phase measurement system is discussed, the basic reason for the existence of high-order spectra components in the frequency domain is analyzed, and the basic method used to reduce the nonlinear effect and separate fundamental frequency information is given. Then, on the basis of reducing the nonlinear effect's influence on the system, the basic principle of phase measurement for the fringe image of a measured object using the dual-frequency grating method is analyzed. To verify the correctness and effectiveness of the proposed phase measurement method, a computer simulation and a practical experiments were implemented with good results. In the simulation, the error value of this method was 27.97% for the method with nonlinear influence, and 52.51% for that with almost no nonlinear influence. In the experiment, the effect of phase recovery produces the best results. This shows that the proposed phase measurement method is effective with a small error.

**Key words:** phase measurement; dual-frequency grating; system nonlinear effect; phase-shift; high-order spectra

## 非线性系统中双频光栅相位测量

乔闹生<sup>1,2\*</sup>, 尚雪<sup>2</sup>

(1. 湖南文理学院 国际学院, 湖南 常德 415000;

2. 湖南文理学院 数理学院, 湖南 常德 415000)

**摘要:** 为了在非线形测量系统中获得更好的相位测量结果, 提出了一种在几乎消除非线性影响后使用双频光栅投影的相位测量方法。首先, 讨论了相位测量系统的非线性效应, 分析了频域中存在高阶频谱成份的基本原因, 给出了减小非线性效应并分离基频信息的基本方法。然后, 在减小系统非线性效应影响的基础上, 分析了使用双频光栅投影测量被测物体条纹图像的相位基本原理。为验证所提出的相位测量方法的有效性, 进行了计算机仿真和实际实验, 获得了良好结

收稿日期: 2022-08-17; 修订日期: 2022-09-19

基金项目: 湖南省教育厅科学研究重点项目(No. 22A0484); 国家自然科学基金(No. 12104150)

Supported by Key Scientific Research Project of Hunan Provincial Department of Education (No. 22A0484);  
National Natural Science Foundation of China (No. 12104150)

果。在仿真实验中,该方法的误差值为有非线性影响方法的 27.97%,为几乎没有非线性影响方法的 52.51%;在实际实验中,该方法的相位恢复效果最好。表明采用本文方法所测量的相位效果好,误差较小。

**关键词:** 相位测量; 双频光栅; 系统非线性效应; 相移; 高阶频谱

中图分类号: O438.2

文献标志码: A

doi: 10.37188/CO.EN.2022-0013

## 1 Introduction

Phase measurement is very important in optics shape measurement. For its non-contact operation, high precision, high speed and other measurement advantages, it is widely used in production, national defense, scientific research and other fields<sup>[1-6]</sup>. Numerous scholars have studied phase measurement and obtained good results<sup>[1-3]</sup>. For example, in 2020, to better measure isolated targets with complex surfaces, Cai *et al.* improved the measurement method of the absolute phase by using half-cycle correction and proposed a new gray coding method<sup>[1]</sup>. In 2021, in order to optimize phase measurement, Peng *et al.* proposed a sine fringe generation technique for three-dimensional shape measurement<sup>[2]</sup>. In 2022, to improve the reliability of tri-frequency time phase unwrapping, Hou *et al.* proposed a method using spatiotemporal tri-frequency time phase unwrapping<sup>[3]</sup>.

Due to the nonlinear effect of the measurement system, phase measurement will be adversely affected. To reduce or even eliminate the nonlinear effect influence and improve measurement accuracy, some scholars have studied it and made some good achievements<sup>[7-11]</sup>. In 2013, to correct the system's gamma nonlinearity, Xiao *et al.* presented a single orthogonal sinusoidal grating used in phase measurement, where the fringe gained by projecting the grating has good sinusoidal properties and can decrease the phase sinusoidal error<sup>[7]</sup>. In 2015, to decrease the phase measurement error induced by the system's gamma nonlinearity, Xu *et al.* corrected the fringe using the system response function<sup>[8]</sup>. In 2021, for the three-step phase-shifting profilometry based nonlinear effect, Yang *et al.* proposed a method to reduce phase error with a three-to-three deep

learning framework<sup>[9]</sup>.

In this paper, the causes of the nonlinear effect influencing fringe intensity in the measurement system and its influence are analyzed in detail. After the nonlinear effect is reduced, the advantages of the dual-frequency grating method are used to gain better phase information of the measured object fringe image, and analyze its principle. To verify the principle analysis, a computer simulation and a practical experiment are executed, whose results show that the principle is correct.

## 2 Principle analysis

### 2.1 Nonlinear effect of system in phase measurement

Phase measurement is very common in optics shape measurement. A diagram of the system's structure and its corresponding parameters are described in Fig. 1 of the literature [12].

In ideal conditions, the light intensity of deformed fringe outputted from the projector system and that inputted to CCD<sup>[13]</sup> is linear. The light intensity image of the sinusoidal fringe from the projector system output is gained by CCD, as shown in the following expression:

$$g(x, y) = a(x, y) + b(x, y) \cos[2\pi f_0 x + \phi(x, y)] \quad , \quad (1)$$

where  $a(x, y)$  indicates the background light field of the stripe,  $b(x, y)$  indicates stripes contrast,  $f_0$  indicates grating fundamental frequency, and  $\phi(x, y)$  indicates phase information.

Fourier transform is executed to the light intensity of the fringe along the  $x$  axis. In the frequency domain, the zero-order spectrum components are eliminated by using the  $\pi$  phase-shift technology<sup>[14]</sup>. The spectra expression containing the height information  $h(x, y)$  of the object can be

gained as follow:

$$G(f_x, f_y) = Q(f_x - f_0, f_y) + Q^*(f_x + f_0, f_y) \quad , \quad (2)$$

where  $f_x$  and  $f_y$  are spatial frequencies along the  $x$  and  $y$  axes, respectively. As seen in Eq. (2), the spectra only contain the fundamental frequencies component of object height information.

By filtering the fundamental frequency component of Eq. (2) and performing an inverse Fourier transform,  $h(x, y)$  can be gained, and  $\phi(x, y)$  can be recovered. The structural parameters of the measurement system are  $L_0$  and  $d^{[15]}$ , when  $L_0 \gg h(x, y)$  in practical situations, the relationship between  $\phi(x, y)$  and  $h(x, y)$  is<sup>[14]</sup>

$$\phi(x, y) = -\frac{2\pi f_0 d}{L_0} h(x, y) \quad . \quad (3)$$

However, owing to the effects of light illumination, external noise and so on, in real situations, the light intensities of the deformed fringes of the projector systems and that of the CCD input is nonlinear, so the light intensity of the deformed fringe passing through the nonlinear projection system is:

$$g'(x, y) = [g(x, y)]^\gamma = \sum_{k=0}^{\infty} a_k \cos\{k[2\pi f_0 x + \phi(x, y)]\} \quad , \quad (4)$$

where  $a_k$  represents the Fourier coefficient,  $k$  is the harmonic component to the order of  $g'(x, y)$ , and  $\gamma$  is the system's gamma value.

A Fourier transform is executed with Eq. (4). Similarly, after eliminating the zero-order spectrum components in the frequency domain by using the  $\pi$  phase-shift technology<sup>[14]</sup>, the frequency domain expression of Eq. (4) becomes:

$$G'(f_x, f_y) = \sum_{k=1}^{\infty} Q_k(f_x - kf_0, f_y) + \sum_{k=1}^{\infty} Q_k^*(f_x + kf_0, f_y) \quad . \quad (5)$$

It can be seen that when there is a nonlinear relationship in the system, there are higher-order spectra components in the frequency domain of the deformed fringe after the Fourier transform. Mixing the fundamental frequency with higher-order spectra components easily leads to spectra overlapping,

which affects the phase measurement accuracy.

The phase information is contained in the fundamental frequency part  $Q_1(f_x - f_0, f_y)$  and  $Q_1^*(f_x + f_0, f_y)$  of the spectra domain. After the low-pass filter is used to filter out the high-order spectra components, almost all of the fundamental frequency components in the frequency domain are obtained, so the nonlinear effect of the system is greatly reduced. The spectra expression gained can be shown as

$$G^\wedge(f_x, f_y) = Q_1(f_x - f_0, f_y) + Q_1^*(f_x + f_0, f_y) \quad . \quad (6)$$

## 2.2 Phase measurement with dual-frequency grating

After the system nonlinear effect is nearly eliminated, the  $n$ -th sinusoidal fringe light intensity image outputted by the measurement system is gained through a CCD as follows:

$$g_n^\wedge(x, y) = F^{-1}[G^\wedge(f_x, f_y)] = \sum_{k=0}^{\infty} A_k^\wedge \cos\{k[2\pi f_0 x + \phi(x, y) + \delta_n]\} \quad , \quad (7)$$

where  $F^{-1}[\cdot]$  represents the inverse Fourier transform,  $A_k^\wedge$  represents the Fourier coefficient of  $g_n^\wedge(x, y)$ , and  $\delta_n$  is the phase-shift amount,  $\delta_n = 2n\pi/n_1$ ,  $n = 1, 2, \dots, n_1$ .

Using the  $n$ -step phase-shift method, the phase gained can be described as

$$\phi^\wedge(x, y) = \arctan \left[ \frac{\sum_{n=1}^N g_n^\wedge(x, y) \sin(\delta_n)}{\sum_{n=1}^N g_n^\wedge(x, y) \cos(\delta_n)} \right] \quad , \quad (8)$$

where  $\phi^\wedge(x, y)$  represents the wrapped phase.

As  $\phi^\wedge(x, y)$  is discontinuous, the phase unwrapping must be executed to gain the continuous unwrapped phase  $\phi(x, y)$ . Their corresponding relationship is

$$\phi(x, y) = \phi^\wedge(x, y) + 2k(x, y)\pi \quad , \quad (9)$$

where  $k(x, y)$  is the integer number that represents the fringe orders.

The phase is easy to unwrap by using the low-

frequency grating, but this has low phase accuracy. One will gain high phase accuracy by using a high-frequency grating, but the phase is then difficult to unwrap. A dual-frequency grating can make full use of both advantages, so a high-precision recovery phase can be achieved<sup>[16]</sup>.

When a dual-frequency grating is used to measure phase, Eq. (9) can be further changed into the following expression:

$$\begin{cases} \phi_h(x,y) = \phi_h^\wedge(x,y) + 2k_h(x,y)\pi \\ \phi_l(x,y) = \phi_l^\wedge(x,y) + 2k_l(x,y)\pi \end{cases}, \quad (10)$$

where “h” represents high-frequency grating, and “l” represents low-frequency grating.

By further changing Eq. (10), it can evolve to Eq. (11) as follows:

$$k_h(x,y) = (INT)\left\{\frac{f_h}{f_l}k_l(x,y) + \frac{1}{2\pi}\left[\frac{f_h}{f_l}\phi_l^\wedge(x,y) - \phi_h^\wedge(x,y)\right]\right\}, \quad (11)$$

where  $(INT)\{\cdot\}$  denotes the integer operator, and  $f_h$  and  $f_l$  represent the fundamental frequency of the high-frequency grating and low-frequency grating, respectively.

So  $k_h(x,y)$  can be decided by  $k_l(x,y)$ ,  $f_l$ ,  $f_h$ ,  $\phi_l^\wedge(x,y)$  and  $\phi_h^\wedge(x,y)$ . The phase  $\phi_h(x,y)$  can be gained from Eq. (10), so  $\phi(x,y)$  can be further obtained.

### 3 Computer simulation and experiment

#### 3.1 Computer simulation

Supposing that the geometric parameters relationship of the phase measurement system is  $L_0/d = 2.5$ , the frequency rate is then  $f_h/f_l = 4$ . The computer-simulated phase is shown in Fig. 1 with a resolution of  $512 \times 512$  pixels.

There is a nonlinear effect in the system, assuming that  $\gamma = 1.23$  in Eq. (4). A Fourier transform is executed along the  $x$ -axis aimed to the light intensity of the deformed fringe. The  $\pi$  phase-shift technique<sup>[14]</sup> is applied to eliminate the zero-order

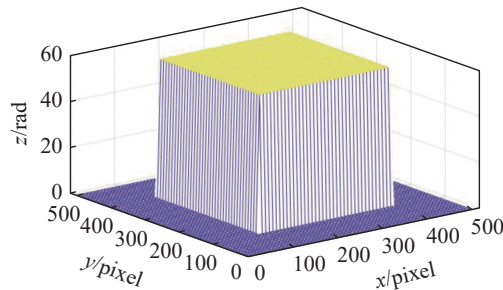
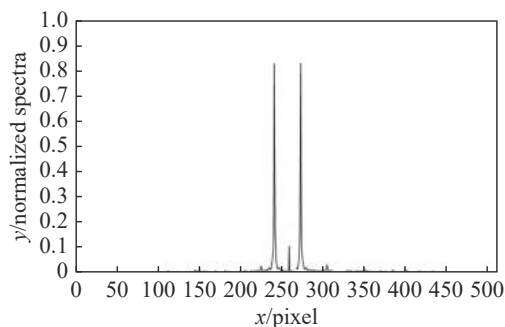
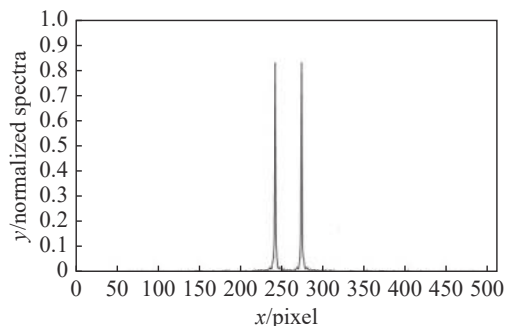


Fig. 1 Simulated phase

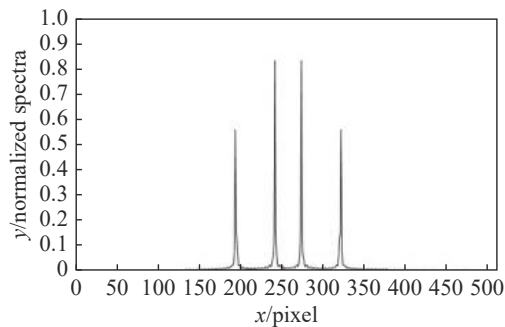
spectrum component of the frequency domain. The spectra distributions gained are shown in Fig. 2 (a). It can be seen that the spectra distributions contain high-order spectra components. After the nonlinear influence of the system is nearly eliminated, the results have nearly no high-order spectra components



(a) With nonlinear effect



(b) Nearly without nonlinear effect



(c) The proposed method's results

Fig. 2 Spectra distributions along  $x$  axis

as shown in Fig. 2 (b). On the basis of there being nearly no nonlinear effect, the spectra distribution obtained by the dual-frequency grating method contains only the fundamental frequency components of the two gratings, as shown in Fig. 2 (c).

After applying the inverse Fourier transform to these spectra distributions as shown in Fig. 2, the gained measurement errors between the recovery phase and the original phase by using the three methods as shown in Figs. 3 (a)–(c) (color online), respectively.

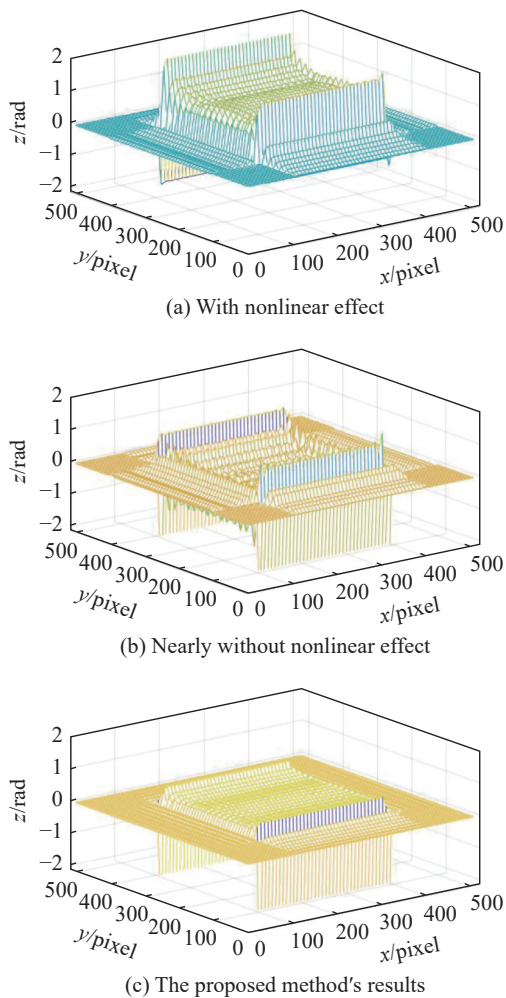


Fig. 3 Phase measurement error diagrams gained by three different simulation methods

The average phase error value of Fig. 3 (a), 3(b) and 3(c) is 0.8452 rad, 0.4438 rad and 0.2364 rad, respectively. The error value of this method is 27.97% and 52.51% that of the method with a nonlinear effect and nearly completely without nonlinear influence, respectively.

The phase in the nonlinear measurement system can be recovered effectively by using the proposed method and its phase recovery error is the smallest among the three methods.

### 3.2 Actual experiment

To further prove the correctness and feasibility of the principle analysis, the actual experiment was executed by using the experimental system shown in Fig. 4. Through a program generated by MATLAB software,  $f_h/f_l = 4$  can be gained.

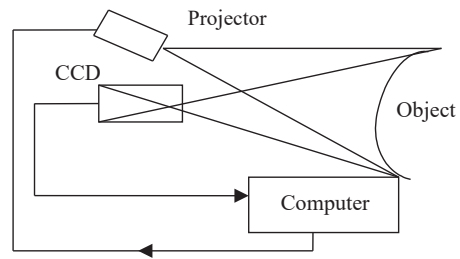


Fig. 4 The structural frame for the experimental device

The experimental model used is a steep stepped object, as shown in Fig. 5 (color online).



Fig. 5 The experiment model used in the experiment

In the experiment, the same three methods of computer simulation are used to measure the phase. The recovery results gained can be shown in Fig. 6 (a), 6(b) and 6(c) (color online), respectively. Fig. 6 (d) is the cross-section comparison results of 100th column of Fig. 6 (a) ~ (c), respectively.

It indicates that the phase measurement result using the method proposed in this paper is best, and the gained phase surface contour is complete and smooth.

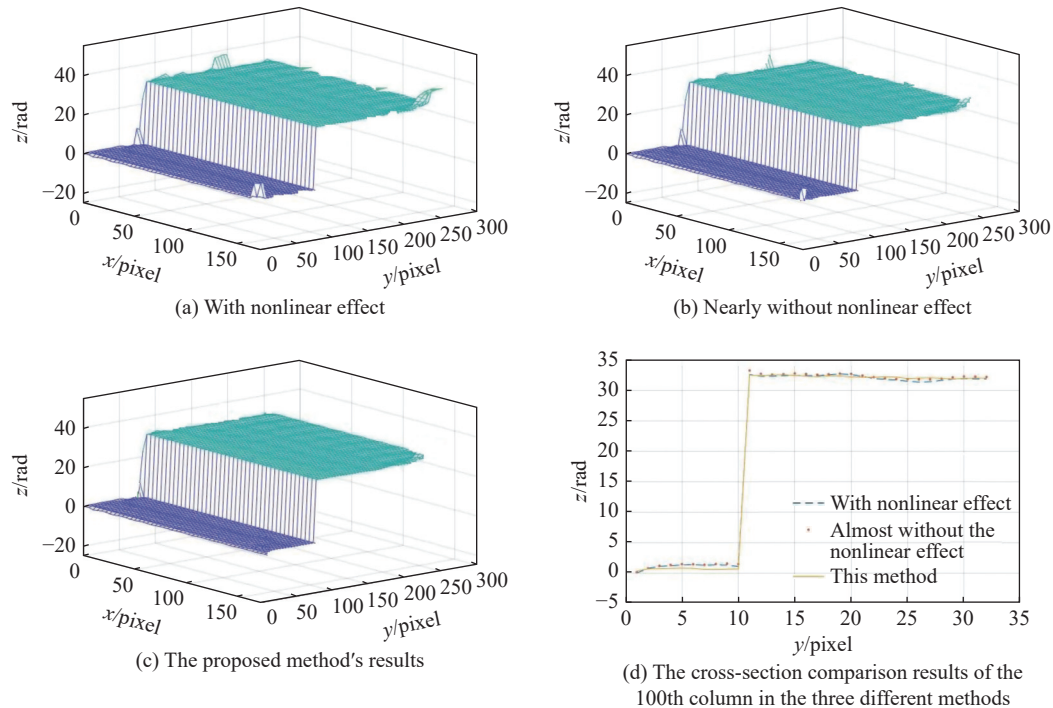


Fig. 6 Phase measurement results gained by using the three different experiment methods

## 4 Conclusion

Due to the influence of the nonlinear effect on phase measurement, the influence of the nonlinear effect on fringe intensity in the measurement system is analyzed. The dual-frequency grating method is used to improve the phase measurement accuracy, and the principle is analyzed.

To verify the effectiveness of the proposed

principle analysis, the computer simulation and practical experiment are implemented, and the results gained are consistent with the principle analysis. The error values of this method by simulation are 27.97% and 52.51% of the methods with and nearly without nonlinear influence, respectively, showing that the effect of phase recovery is the best among those in the experiment. This demonstrates that the phase measurement method proposed in this paper is effective and feasible.

## References:

- [1] CAI B L, YANG Y, WU J, *et al.*. An improved gray-level coding method for absolute phase measurement based on half-period correction[J]. *Optics and Lasers in Engineering*, 2020, 128: 106012.
- [2] PENG R J, TIAN M R, XU L, *et al.*. A novel method of generating phase-shifting sinusoidal fringes for 3D shape measurement[J]. *Optics and Lasers in Engineering*, 2021, 137: 106401.
- [3] 侯艳丽, 梁瀚钢, 李付谦, 等. 相位测量轮廓术中时空结合的三频相位展开[J]. *光学学报*, 2022, 42(1): 0112006.
- [4] HOU Y L, LIANG H G, LI F Q, *et al.*. Spatial-temporal combined phase unwrapping in phase measurement profilometry[J]. *Acta Optica Sinica*, 2022, 42(1): 0112006. (in Chinese)
- [5] QIAO Z K. Study for phase retrieval based on dual frequency grating projection[J]. *Optik*, 2021, 245: 167668.
- [6] 张旭, 邵双运, 祝祥, 等. 光学三维扫描仪光强传递函数的测量和校正[J]. *中国光学*, 2018, 11(1): 123-130.
- [7] ZHANG X, SHAO SH Y, ZHU X, *et al.*. Measurement and calibration of the intensity transform function of the optical 3D profilometry system[J]. *Chinese Optics*, 2018, 11(1): 123-130. (in Chinese)
- [6] YIN W, HU Y, FENG SH J, *et al.*. Single-shot 3D shape measurement using an end-to-end stereo matching network for speckle projection profilometry[J]. *Optics Express*, 2021, 29(9): 13388-13407.
- [7] XIAO Y SH, CAO Y P, WU Y CH, *et al.*. Single orthogonal sinusoidal grating for gamma correction in digital

- projection phase measuring profilometry[J]. *Optical Engineering*, 2013, 52(5): 053605.
- [8] YE X, CHENG H B, WU H Y, *et al.*. Gamma correction for three-dimensional object measurement by phase measuring profilometry[J]. *Optik*, 2015, 126(24): 5534-5538.
- [9] YANG Y, HOU Q Y, LI Y, *et al.*. Phase error compensation based on Tree-Net using deep learning[J]. *Optics and Lasers in Engineering*, 2021, 143: 106628.
- [10] KAMAGARA A, WANG X ZH, LI S K. Towards gamma-effect elimination in phase measurement profilometry[J]. *Optik*, 2018, 172: 1089-1099.
- [11] 李东林, 曹益平. 一种基于背景校正的2+1相移算法[J]. *光子学报*, 2019, 48(4): 0415001.  
LI D L, CAO Y P. 2+1 phase-shifting algorithm based on background correction[J]. *Acta Photonica Sinica*, 2019, 48(4): 0415001. (in Chinese)
- [12] 乔闹生, 孙萍. CCD非线性效应对双频光栅三维面形测量的影响[J]. *中国光学*, 2021, 14(3): 661-669.  
QIAO N SH, SUN P. Influence of CCD nonlinearity effect on the three-dimensional shape measurement of dual frequency grating[J]. *Chinese Optics*, 2021, 14(3): 661-669. (in Chinese)
- [13] 杜明鑫, 闫钰锋, 张燃, 等. 基于透镜阵列的三维姿态角度测量[J]. *中国光学*, 2022, 15(1): 45-55.  
DU M X, YAN Y F, ZHANG R, *et al.*. 3D position angle measurement based on a lens array[J]. *Chinese Optics*, 2022, 15(1): 45-55. (in Chinese)
- [14] LI J, SU X Y, GUO L R. Improved Fourier transform profilometry for the automatic measurement of three-dimensional object shapes[J]. *Optical Engineering*, 1990, 29(12): 1439-1444.
- [15] TAKEDA M, MUTOH K. Fourier transform profilometry for the automatic measurement of 3-D object shapes[J]. *Applied Optics*, 1983, 22(24): 3977-3982.
- [16] DAI M L, YANG F J, LIU C, *et al.*. A dual-frequency fringe projection three-dimensional shape measurement system using a DLP 3D projector[J]. *Optics Communications*, 2017, 382: 294-301.

#### Author Biographics:



QIAO Nao-sheng (1971—), Ph.D, Professor, International College, Hunan University of Arts and Science. His research interests are in optical information processing. E-mail: naoshengqiao@163.com